Cell Reports

A ribosome-bound tRNA half stimulates mitochondrial translation during stress recovery in *Trypanosoma brucei*

Graphical abstract

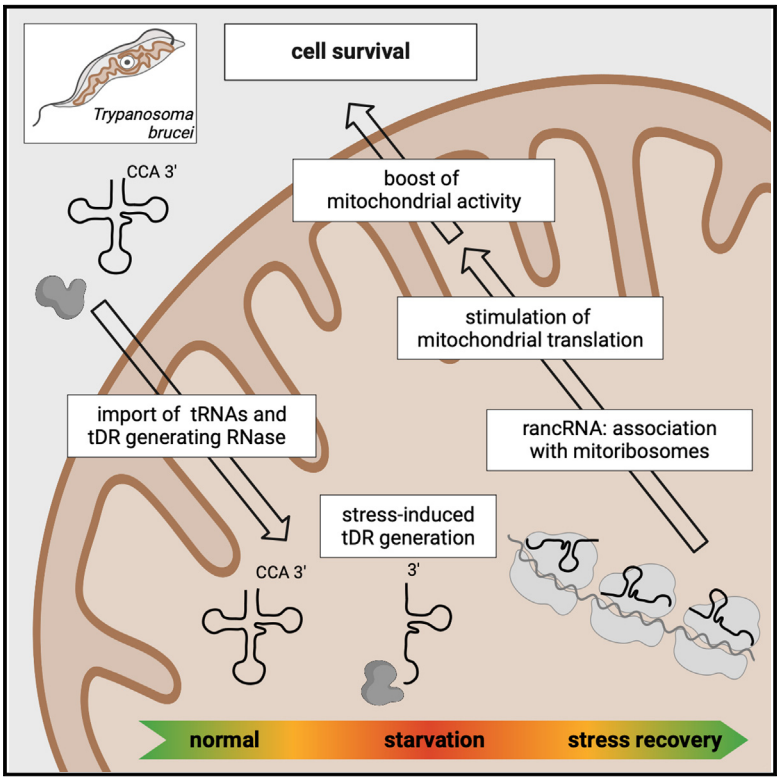

Highlights

- tRNA-derived RNAs accumulate in the mitochondria of *T. brucei* exposed to nutritional stress
- Most tRNA-derived RNAs detected during exponential growth are found in the cytosol
- The enzymatic activity generating tDRs is detected in mitochondria
- $tRNA^{Thr}$-3′-half binds to mitochondrial ribosomes promoting translation and stress survival

Authors

Rebecca Brogli, Marina Cristodero, André Schneider, Norbert Polacek

Correspondence

marina.cristodero@unibe.ch (M.C.), norbert.polacek@unibe.ch (N.P.)

In brief

Brogli et al. describe the mitochondrial localization of several tRNA-derived small RNAs in the parasite *Trypanosoma brucei*. Starvation triggers the generation of the $tRNA^{Thr}$ 3′ half inside the mitochondria, where it associates with mitoribosomes, stimulating organellar translation. This potentially enhances mitochondrial energy production capacity and survival during stress recovery.

Brogli et al., 2023, Cell Reports *42*, 113112
September 26, 2023
https://doi.org/10.1016/j.celrep.2023.113112

CellPress

Cell Reports

CellPress
OPEN ACCESS

Report

A ribosome-bound tRNA half stimulates mitochondrial translation during stress recovery in *Trypanosoma brucei*

Rebecca Brogli,[1,2] Marina Cristodero,[1,3,*] André Schneider,[1] and Norbert Polacek[1,*]
[1]Department of Chemistry, Biochemistry and Pharmaceutical Sciences, University of Bern, 3012 Bern, Switzerland
[2]Graduate School for Cellular and Biochemical Sciences, University of Bern, 3012 Bern, Switzerland
[3]Lead contact
*Correspondence: marina.cristodero@unibe.ch (M.C.), norbert.polacek@unibe.ch (N.P.)
https://doi.org/10.1016/j.celrep.2023.113112

SUMMARY

The protozoan parasite *Trypanosoma brucei* and its disease-causing relatives are among the few organisms that barely regulate the transcription of protein-coding genes. Yet, alterations in its gene expression are essential to survive in different host environments. Recently, tRNA-derived RNAs have been implicated as regulators of many cellular processes within and beyond translation. Previously, we identified the tRNA^{Thr}-3′-half (AGU) as a ribosome-associated non-coding RNA able to enhance global translation. Here we report that the tRNA^{Thr}-3′-half is generated upon starvation inside the mitochondria. The tRNA^{Thr}-3′-half associates with mitochondrial ribosomes and stimulates translation during stress recovery, positively affecting mitochondrial activity and, consequently, cellular energy production capacity. Our results describe an organelle ribosome-associated ncRNA involved in translation regulation to boost the central hub of energy metabolism as an immediate stress recovery response.

INTRODUCTION

Organisms must adapt to challenging environments for survival. This adaptation requires rapid gene expression reprogramming to overcome stress.[1] Mitochondria play a crucial role in orchestrating adaptive stress responses by generating energy through oxidative phosphorylation (OXPHOS). Impaired mitochondrial translation leads to respiratory chain dysfunction and energy deficit.[2–4] *Trypanosoma brucei,* a parasitic protozoon, undergoes complex transitions between two different hosts, a mammal and the tsetse fly.[5] Glucose is the primary energy source for mammalian bloodstream parasites (BSF), while amino acid catabolism sustains the insect procyclic form (PCF). Adjusting to these conditions requires gene expression regulation, primarily through post-transcriptional mechanisms.[6,7] Trypanosomes possess unique RNA characteristics, including polycistronic gene organization, coupled *trans*-splicing and polyadenylation,[8] editing of mitochondrial mRNAs,[9] cytosolic ribosomal large subunits composed of several distinct rRNA fragments,[10] highly divergent mitochondrial ribosomes containing the smallest known rRNAs,[11] and a total lack of mitochondrially encoded tRNAs.[12]

tRNA-derived RNAs (tDRs) are a class of regulatory small non-coding RNAs (ncRNAs) encompassing tRNA halves (≈35 nt) as well as shorter tRNA fragments.[13] tDRs have been identified in all domains of life and have multifaceted functions in regulating transcription, translation, stress granule formation, non-genomically encoded inheritance, and intra- and intercellular communication, among other processes.[14,15]

Several studies described the roles of tDRs in translation regulation. In mammalian cells exposed to oxidative stress, specific 5′-tDRs inhibit global translation by displacing translation initiation factors from mRNAs and inducing stress granule assembly.[16–20] Distinct from the global effect, tDR-5′-Leu binds a complementary sequence on an mRNA coding for a ribosomal protein enhancing its translation and boosting ribosome biogenesis in cancer cells.[21,22] In plants and flies, tDRs were shown to hijack the siRNA pathways to target sequence-specific mRNAs for translation inhibition or by blocking the siRNA pathway.[23–25]

Ribosome-associated ncRNAs (rancRNAs) are another class of riboregulators involved in translation control mechanisms in all domains of life.[26] rancRNAs regulate translation by directly interacting with ribosomes, mainly during stress responses. These molecules differ from proteinaceous translation modulators by their immediate availability since rancRNAs derive from pre-existing molecules such as mRNAs, rRNAs, snoRNAs, and tRNAs.[26] rancRNAs also derive from antisense transcription.[26,27] tDRs are one of the most common and better-studied rancRNAs.[28–30]

Previously, we identified numerous tDRs in *T. brucei* subjected to different growth conditions.[30] The most abundant tDR was a 37 nt long tRNA^{Thr}-3′-half (AGU) lacking the CCA tail (tDR-37:73-Thr-AGU-1).[13,31] This tRNA half accumulated during starvation and remained stable during stress recovery. The tRNA^{Thr}-3′-half

associated with cytosolic ribosomes *in vitro* and *in vivo* stimulating global translation during stress recovery.[30]

Here, we show that starvation-induced tDRs and the enzymatic activity responsible for tDR biogenesis in *T. brucei* are mitochondrial. Notably, the levels of the tRNA^{Thr}-3′-half were increased in mitochondria of nutrient-deprived cells, and the tRNA^{Thr}-3′-half interacted with mitochondrial ribosomes to stimulate protein biosynthesis. This stimulation of mitochondrial translation had a beneficial effect on mitochondrial function and energy capacity during the stress recovery phase.

RESULTS

The tRNA^{Thr}-3′-half localizes to the mitochondria upon starvation

Earlier, we identified the tRNA^{Thr}-3′-half as a genuine rancRNA capable of stimulating cytosolic translation *in vitro* and *in vivo*.[30] Notably, the *T. brucei* tRNA^{Thr}-3′-half also stimulated translation in an archaeal species, yeast, and human cell extracts, thus hinting at a highly conserved ribosome binding site and mode of action.

Due to the absence of tRNA genes in the mitochondrial genome of *T. brucei*,[32] all tRNAs must be imported into mitochondria. Therefore, tRNAs functioning in translation in both cellular compartments are indistinguishable. To assess whether the tRNA^{Thr}-3′-half is present in mitochondria, subcellular localization of the tRNA^{Thr}-3′-half was investigated. Northern blot analyses of crude mitochondrial fractions of exponentially growing or nutritionally stressed PCF showed that the tRNA^{Thr}-3′-half predominantly localized to the mitochondria-enriched fraction (Figure 1A). The tRNA^{Thr}-3′-half was also enriched in purified mitochondria[33] (Figure S1A and S2A), confirming that the tRNA^{Thr}-3′-half is present inside the mitochondrion and not just co-purifying with the crude mitochondrial fraction. Comprehensive northern blot analyses showed that other 5′-derived and 3′-derived tDRs were also present in the mitochondria upon nutritional stress (Figures 1B and S2B). Except for tDR-5′-Val, all tDRs detected under exponential growth in PCF were mainly detected in the cytosolic fraction (tDR-5′-Ala, tDR-5′-Lys, tDR-5′-Tyr; Figure 1B). Nutritional stress triggered an increase in tDR-5′-Glu and tDR-5′-Val levels of mitochondrial fragments without altering the cytosolic signal. The tDR-3′-Tyr was only detected in the cytosol during exponential growth, while it appeared to be only present in the mitochondria during nutritional stress.

Similar to PCF, the tRNA^{Thr}-3′-half accumulated in the mitochondria of BSF (Figure 1A). In BSF all the tRNA halves tested were mainly detected in mitochondrial fractions (Figures 1A and S2B). These data indicate that tDR localization is not only life stage and stress condition dependent, but also tDR-specific.

tRNA^{Thr}-3′-halves are generated inside the mitochondria

The RNase(s) responsible for tDR biogenesis in trypanosomes are unknown. Some well-described RNases involved in tRNA halves generation, namely mammalian angiogenin and yeast Rny1, are constitutively present in cells and only activated in the cytosol under certain conditions.[20,34] To test if this is also the case in trypanosomes, the generation of tRNA^{Thr}-3′-half on total cell lysates was investigated. Figure 2A shows a substantial increase in tRNA^{Thr}-3′-half levels with time, suggesting that the processing activity is constitutively present but kept inactive under exponential growth conditions. Treatment of cell lysates with a broad-spectrum RNase inhibitor abolished tRNA processing, suggesting the involvement of a proteinaceous enzyme (Figure 2B).

To test if the tRNA^{Thr}-3′-half is produced inside mitochondria, mitochondria lysates were incubated with *T. brucei* total RNA. Indeed, mitochondrial lysates were capable of generating tRNA^{Thr}-3′-halves (Figure 2C), suggesting that this tDR is generated inside the organelle subsequent to tRNA import. Support for this conclusion comes from experiments where ATOM40, the main component of the protein import machinery, was depleted (Figure 2D). This resulted in an increase in the levels of cytosolic tRNA^{Thr}-3′-halves probably due to the mislocalization of the putative tDR-generating RNase (Figure 2E). tDR-5′-Ala served as specificity control since this tDR was not detected inside mitochondria.

To identify the enzyme responsible for tRNA processing, we performed activity-guided biochemical fractionations followed by mass spectroscopy analysis of fractions showing *in vitro* tRNA processing activity. RNAi against 33 candidates failed to uncover the enzyme responsible for tRNA^{Thr}-3′-half processing (Table S2). Taken together, these experiments strengthen the view of a mitochondrial tRNA half generated inside the organelle by a so far unidentified RNase.

The tRNA^{Thr}-3′-half associates with mitoribosomes

Since the endogenous *T. brucei* tRNA^{Thr}-3′-half is present in mitochondria, we next investigated whether this tDR binds to mitochondrial ribosomes (mitoribosomes). For this, mitochondria lysates were fractionated, and the obtained pellet containing heavy ribonucleoprotein particles (mitP100) was further separated over sucrose gradients (Figure S1C) to isolate mitoribosomal particles. Analysis of RNA extracted from selected fractions indicated the presence of tRNAs in the lighter fractions (peaks A and B) and mitoribosomal RNAs (12S and 9S rRNAs) in the heavier part of the gradient (peaks C and D; Figure S1D). Western blot analysis showed the successful separation of light proteins and editosome complexes (peak A and B, respectively) from mitoribosomes (Figure S1E).

To evaluate if the tRNA^{Thr}-3′-half associates with mitoribosomes, we performed *in vitro* binding studies using purified *T. brucei* mitoribosomes or cytosolic 80S ribosomes (Figure 3A). The tRNA^{Thr}-3′-half not only bound to cytosolic ribosomes but also to mitoribosomes (Figure 3B). To investigate binding *in vivo*, mitoribosomes were immunoprecipitated from cells expressing a PTP-tagged mitoribosomal protein[11] (uL3m, Tb927.3.5610, Figures S1F and 3C). Indeed, the tRNA^{Thr}-3′-half interacted with mitochondrial ribosomes also *in vivo* (Figure 3D). The tDR-5′-Trp and tDR-3′-Tyr, two mitochondrial tDRs that do not interact with ribosomes,[30] failed to co-purify with the mitoribosomes (Figure 3D), highlighting the specificity of the interaction of the tRNA^{Thr}-3′-half with mitoribosomes.

To further substantiate these findings, mitochondrial lysates were incubated with tRNA^{Thr}-3′-halves in the presence or

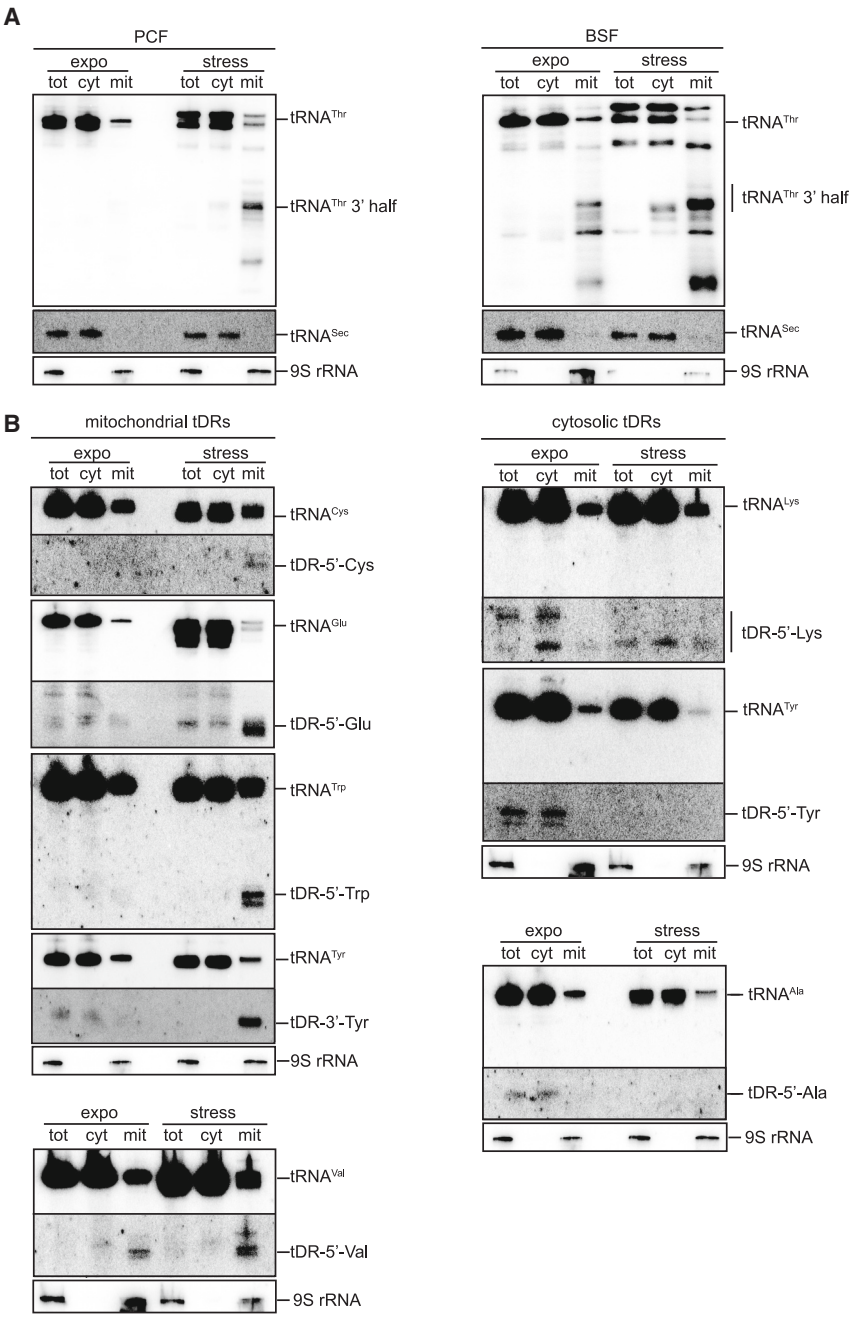

Figure 1. tRNA^{Thr}-3′-half localizes to the mitochondria in the procyclic and bloodstream forms of *T. brucei*

(A) Procyclic (PCF) or bloodstream form (BSF) parasites were grown exponentially (expo) or nutritionally stressed (stress) and the presence of the tRNA^{Thr}-3′-half in whole cells (tot), soluble fractions (cyt) and mitochondria-enriched pellets (mit) was monitored by northern blot analysis. tRNA^{Sec} and 9S rRNA serve as cytosolic and mitochondrial markers, respectively.

(B) The localization of various tDRs was investigated as in (A). The lower panel displays the respective tDR with an increased contrast. In all cases, the relative amounts are 1x for total and cytosolic fractions and 19x for mitochondria-enriched pellets. Controls are as in (A) and were re-used when the same membrane was hybridized with different probes for easier comparison.

absence of EDTA prior to their loading on sucrose gradients. In the absence of the chelator, the tRNA^{Thr}-3′-half was detected in fractions containing mitochondrial ribosomes and polysomes (Figures S3A and S3B). Importantly, upon EDTA treatment, a decrease in ribosomes and a concomitant decrease in the tRNA^{Thr}-3′-half signal in the heavy fraction was observed, together with an increase in the amount of tRNA^{Thr}-3′-half comigrating with the dissociated mitoribosomal subunits (Figure S3B). Taken together, these data demonstrate that both synthetic and endogenous mitochondrial tRNA^{Thr}-3′-halves associate with mitoribosomes *in vitro* and *in vivo*.

tRNA^{Thr}-3′-halves stimulate mitochondrial translation

Having established the association of the tRNA^{Thr}-3′-half with mitochondrial ribosomes, we next tested whether this interaction also affected mitoribosomes' performance. For this purpose, a previously reported *in vivo* mitochondrial translation assay was established.[35] Briefly, cells were grown in media supplemented with ^{35}S-methionine and ^{35}S-cysteine and cytosolic translation was inhibited using cycloheximide. Mitochondria were then isolated, and proteins were separated using two-dimensional denaturing gel electrophoresis. The remaining cytosolic proteins migrated in the diagonal of the gel, whereas the mitochondrially translated Cox1 and CytB migrated slightly above (Figure 4A). Knockdown of the mitochondrial translation factor EF-Tu[36] resulted in a strong decrease of CytB and Cox1 signals, showing that we were indeed detecting mitochondria translation (Figure 4A).

During starvation, *T. brucei* rapidly downregulates cytosolic translation.[30,37,38] To analyze the effect of starvation on mitochondrial translation, we followed mitochondrial translation during stress recovery. As seen in Figure 4B, the *de novo* synthesis of Cox1 and CytB was drastically reduced during recovery from starvation.

To study the effect of the tRNA^{Thr}-3′-halves on mitochondrial protein synthesis, we first investigated whether the *in vitro* transcribed tRNA halves can be delivered into *T. brucei* mitochondria via electroporation. Figure S4A shows that approximately 12,000 molecules of tRNA^{Thr}-3′-half were successfully electroporated per cell of which approximately 5,600 were present inside the single mitochondrion. These numbers are in the same order of

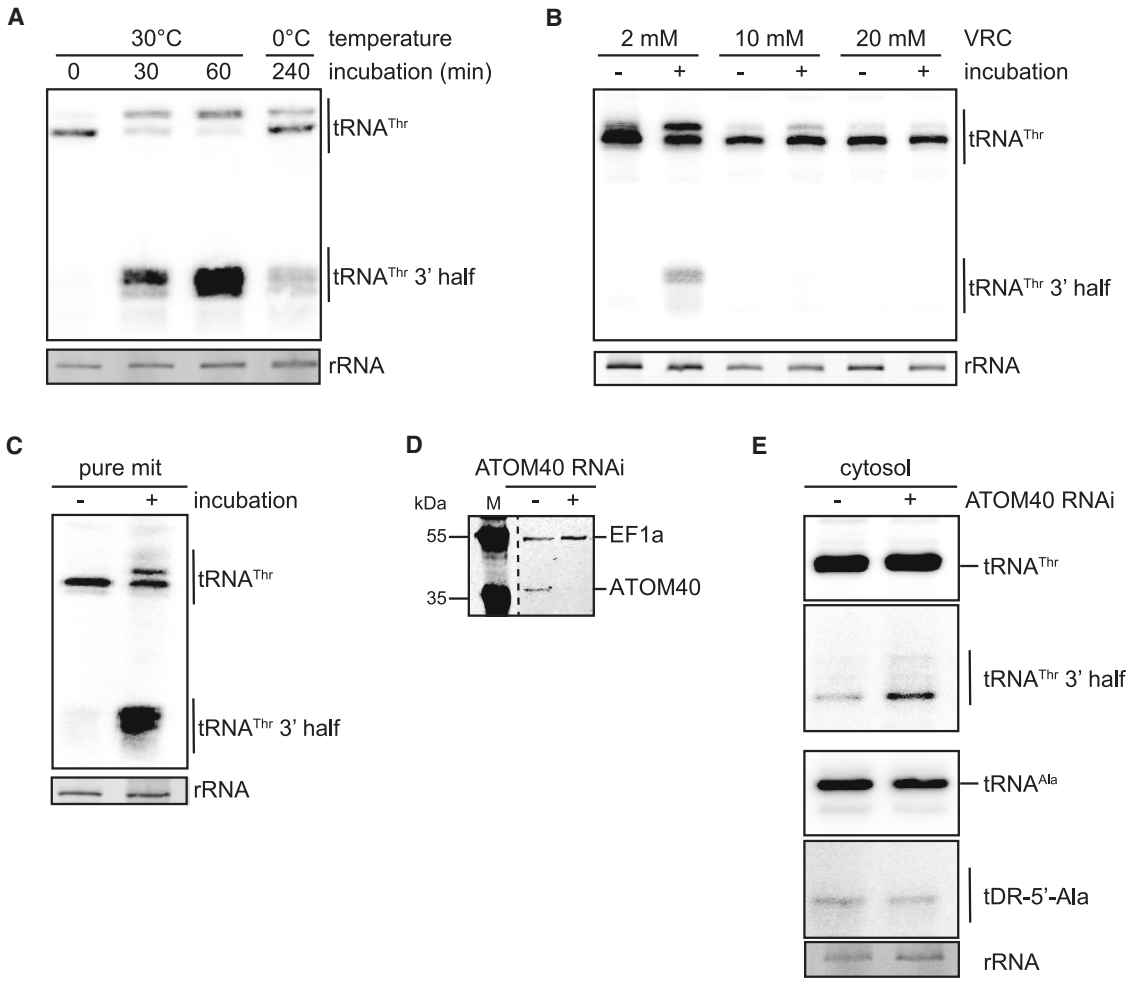

Figure 2. The RNase generating the tRNA^{Thr}-3′-half is constitutively expressed in mitochondria

(A) Total lysates from exponentially growing PCF were incubated at 30°C or 0°C for the indicated times and the levels of the tRNA^{Thr}-3′-half were analyzed by northern blot. The 0 min time serves as a control.

(B) Cell lysates were treated with different concentrations of vanadyl ribonucleoside complex (VRC), incubated at 30°C for 30 min, and tRNA^{Thr}-3′-half levels tested as in (A).

(C) Mitochondrial lysates were incubated with total RNA at 30°C for 30 min. tRNA^{Thr}-3′-half biogenesis was tested by northern blot analysis as before.

(D) The levels of ATOM40 in cells uninduced (−) or induced for RNAi (+) were analyzed by western blotting. EF1a serves as loading control. M, molecular weight marker.

(E) Subcellular fractionation of cells uninduced or induced for ATOM40 RNAi was performed as described and the levels of tRNA^{Thr}-3′-half and tDR-5′-Ala were investigated by northern blot analysis. In all figures, the lowest panel shows the ethidium bromide-stained rRNAs.

magnitude as the endogenous levels of tRNA^{Thr}-3′-halves detected upon starvation.[30] In the presence of electroporated tRNA^{Thr}-3′-halves, a significant increase of up to 67% in mitochondrial protein synthesis was observed during stress recovery (Figures 4C and 4D). Consistently, blocking the endogenous tRNA^{Thr}-3′-half with antisense oligonucleotides (ASO) resulted in an inhibition of mitochondrial translation of around 40% (Figures 4C and 4D).

Most mitochondrially translated proteins are subunits of high molecular weight complexes involved in OXPHOS. Therefore, changes in mitochondrial translation might affect cellular respiration. To analyze whether newly translated mitochondrial proteins can be detected in these complexes, we performed blue native-polyacrylamide gel electrophoresis of mitochondria isolated after ^{35}S *in vivo* labeling during stress recovery. Indeed, newly translated proteins were detected in high molecular weight complexes in mitochondria (Figure S4B). Given the role of mitochondria-translated proteins in energy production, we explored the tDR's influence on metabolism and viability using the MTT assay. Reduction of the tetrazolium dye MTT is catalyzed by mitochondrial dehydrogenases (NADH-dehydrogenase complex I, succinate dehydrogenase, lactate, and malate dehydrogenase)[39] and therefore this assay directly assesses mitochondrial activity. tRNA^{Thr}-3′-half electroporation resulted in a mild yet significant increase in MTT-formazan production suggesting a beneficial effect of the tDR on survival (Figure 4E). No effect in mitochondria activity was observed upon electroporation of the tDR-5′-Ala, a tDR that does not affect translation[30] (Figure 4E).

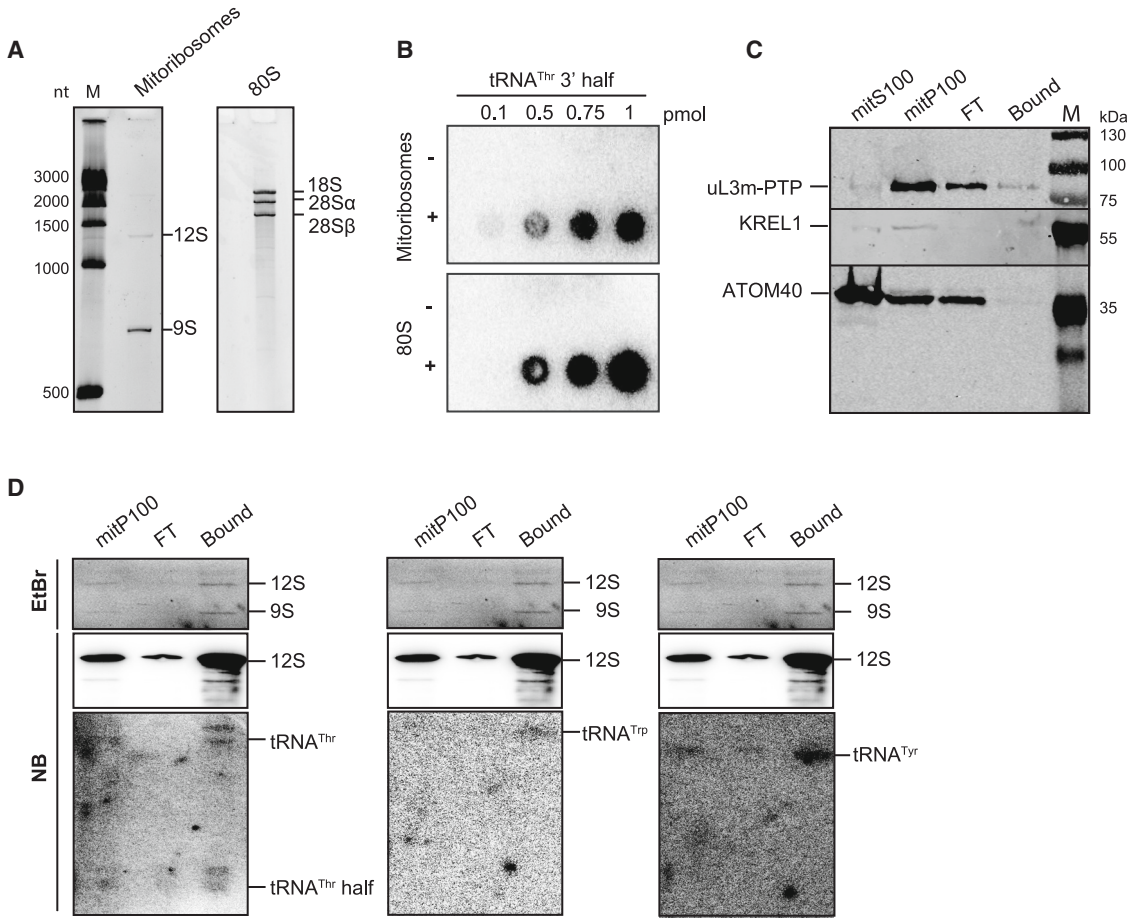

Figure 3. tRNA^{Thr}-3′-half associates with procyclic *T. brucei* mitoribosomes

(A) RNA was extracted from mitoribosomes and cytosolic 80S ribosomes, and run on a denaturing polyacrylamide gel followed by EtBr staining to test their purity.

(B) *In vitro* filter binding assays using equal numbers of ribosomes of either mitoribosomes or 80S ribosomes and increasing amounts of 5′ [^{32}P]-end-labeled tRNA^{Thr}-3′-halves. This representative scan shows one of three experiments.

(C) The presence of the PTP-tagged uL3m (uL3m-PTP) in samples obtained from each immunoprecipitation step was analyzed by western blot. M, molecular weight marker.

(D) The presence of tDRs immunoprecipitated with mitoribosomes was investigated by northern blot analysis. 12S mitochondrial rRNA serves as a marker for mitochondrial ribosomes. Controls were re-used when the same membrane was hybridized with different probes for easier comparison (upper boxes in each panel).

Additionally, mitochondrial membrane potential was monitored *in vivo* using the membrane potential-sensitive dye tetramethylrhodamine ethyl ester (TMRE).[40] Although no significant effect of the tRNA^{Thr}-3′-half in mitochondrial membrane potential was observed (Figure S4C), dramatic changes in cell viability were evident (Figure 4F). tRNA^{Thr}-3′-half resulted in a 25% reduction in the number of dead cells. Importantly, blocking the endogenous tRNA^{Thr}-3′-halves via ASO resulted in a substantial increase in cell death, comparable to inhibiting translation with lethal doses of cycloheximide (Figure 4F).

In summary, these data suggest that *T. brucei* tRNA^{Thr}-3′-halves stimulate mitochondrial translation, thereby boosting overall mitochondrial activity during recovery from nutritional stress. This stimulation results in increased survival rates, providing the parasite with better chances of recovering from stress.

DISCUSSION

Here, we analyzed the effect of nutritional stress on mitochondrial tDR generation and specifically the effect of tRNA^{Thr}-3′-half on organellar translation in the pathogen *Trypanosoma brucei*. With only two exceptions, all previously identified nutritional stress-induced tDRs[30] localize to the mitochondria, whereas most tDRs present in exponentially growing PCF are predominantly cytosolic (Figures 1 and S2).

In PCF, tDRs are generated from many tRNA isoacceptors, and their levels varied depending on the growth conditions.[30] Furthermore, exponentially growing BSF parasites exhibit a different tDR pattern[30] that is also reflected in the subcellular localization of tDRs in this stage (Figures 1A and S2B). The tRNA^{Thr}-3′-half and tDR-5′-Phe are present in BSF regardless of stress and predominantly localize to the mitochondria,

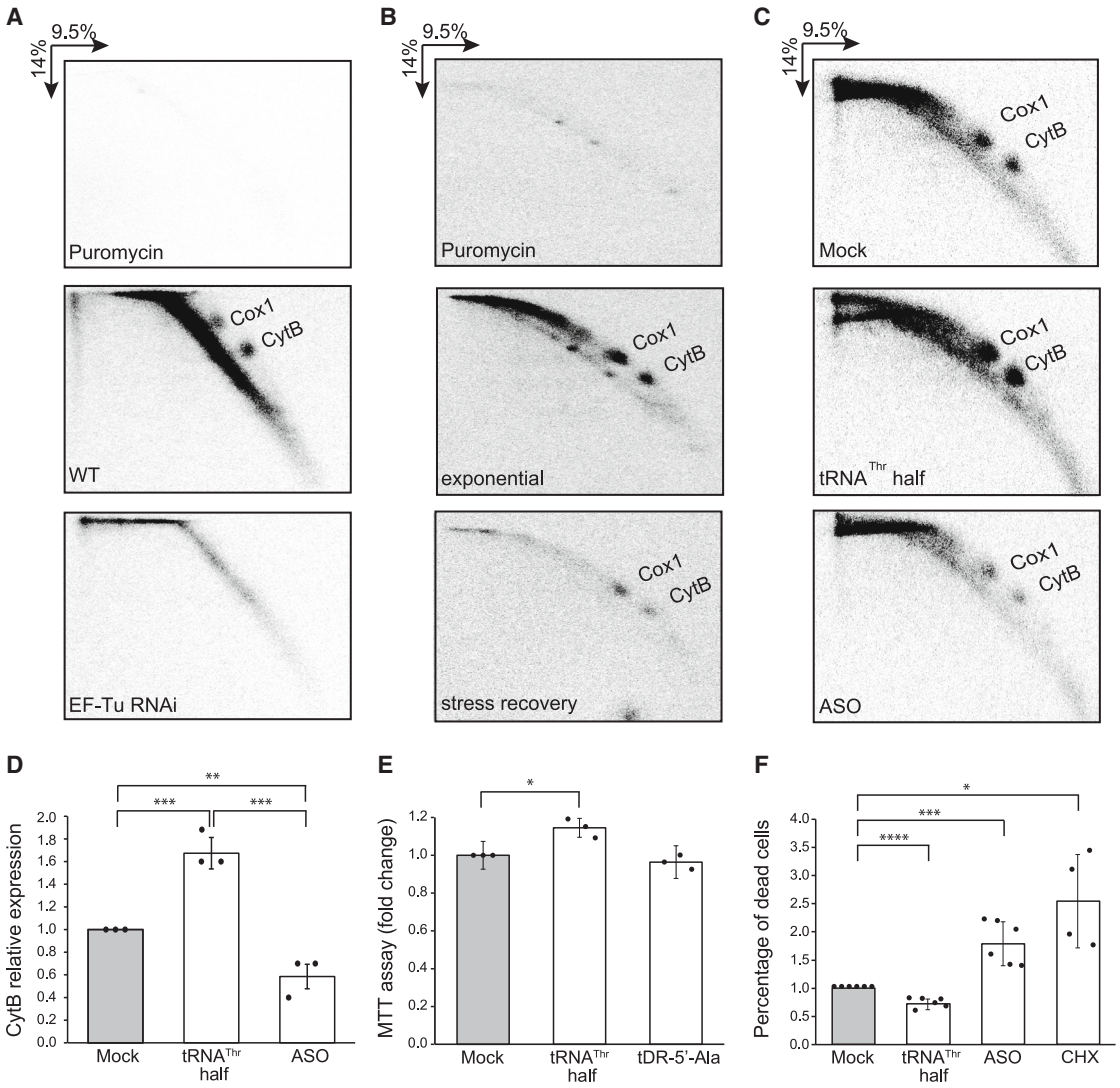

Figure 4. tRNA^{Thr}-3′-half stimulates mitochondrial translation in *T. brucei* procyclic cells *in vivo*

(A) Mitochondrial translation was investigated under standard conditions (WT) or after EF-Tu RNAi induction. Radioactively labeled newly synthesized proteins were resolved by two-dimensional SDS-PAGE electrophoresis. Spots corresponding to CytB and Cox1 are indicated. Puromycin serves as a general translation inhibition control.

(B) Mitochondrial protein synthesis in exponentially growing PCF or during stress recovery was investigated as in (A).

(C) Mitochondrial translation was tested in the absence (Mock) or presence of electroporated tRNA^{Thr}-3′-halves or ASO. Electroporated cells were starved, allowed to recover for 1 h, and translation was analyzed during the second hour of stress recovery, as described in (A).

(D) Quantitative densitometric analysis of *de novo* synthesis of CytB from three independent biological replicates. Values were normalized to mock (n = 3, error bars show standard deviation).

(E) MTT assay of procyclic cells in the absence (Mock) or presence of electroporated tRNA^{Thr}-3′-half or tDR-5′-Ala. Data show the normalized mean values and the standard deviation from three biological replicates.

(F) Measurement of mitochondrial membrane potential in cells electroporated in the absence (Mock) or presence of tRNA^{Thr}-3′-halves, ASO or cells treated with the cytosolic translation inhibitor cycloheximide (CHX). TMRE fluorescence was measured by flow cytometry. The data represent the percentage of dead cells in the sample normalized to dead cells in the mock. Six biological replicates were analyzed, with error bars showing standard deviation. Stars indicate the significance of differences determined by the Student's t test (*$p \leq 0.05$; **$p \leq 0.01$; ***$p \leq 0.001$; ****$p \leq 0.0001$).

whereas in PCF only starvation-induced tDRs are present in the mitochondria (Figures 1A and S2B). The highly distinctive expression and localization patterns of tDRs across different growth stages and stresses suggest physiologically important roles.

Herewith, we provide evidence that mitochondrial tDRs are generated inside the organelle. Incubation of mitochondria lysates with total RNA resulted in the generation of tRNA^{Thr}-3′-halves, demonstrating that the enzyme responsible for tDR biogenesis is localized to the mitochondrion (Figure 2C).

Although the presence of tDRs in different organelles has been previously described, the nucleases responsible for tRNA cleavage remain unknown.[41] In *T. brucei,* the enzyme targeting tRNAs in mitochondria seems to be tightly and differentially regulated during the parasite's life stages and under stress conditions, like the well-known tDR-producing enzymes angiogenin and Rny1. Both RNases are expressed under normal growth conditions but only become active in the cytosol during stress.[17,42,43] A similar inactivation mechanism to protect tRNAs from adverse cleavage appears to operate in trypanosomes. Cell lysates from exponentially growing cells can generate tRNA-3′-halves from $tRNA^{Thr}$, suggesting that the RNase is constitutively present but kept inactive in exponentially growing cells (Figure 2A). It is possible that, in intact cells, not only mitochondria sequestration but also a putative inhibitor is at work. We hypothesize that during stress and upon cell lysis this inhibitor becomes inactive, thereby allowing the activation of the RNase and, as a consequence, tRNA cleavage. Although this is an attractive hypothesis, we cannot exclude that the observed *in vitro* tRNA cleavage activity is non-specific and different from the endogenous one nor that the enzyme(s) is present in other cellular compartments and released upon stress.

Despite our efforts, the identity of the mitochondrial RNase(s) responsible for tDR biogenesis in *T. brucei* remains unknown (Table S2). Analysis of endonuclease V (EndoV; Tb927.10.6860), an RNase shown to cleave inosine-containing tRNAs,[44] retrieved inconclusive data. While overexpression of EndoV resulted in increased levels of tDRs from inosine-containing tRNAs *in vivo* and purified *T. brucei* EndoV catalyzed the cleavage of $tRNA^{Thr}$ *in vitro*, knockdown of EndoV did not significantly reduce the levels of these tDRs in PCF (Figure S5). This discrepancy may be explained by multiple redundant RNases contributing to tDR biogenesis or EndoV not being the primary enzyme responsible for *in vivo* tDR production.

In our previous study, we demonstrated that the starvation-induced $tRNA^{Thr}$-3′-half functions as a *bona fide* rancRNA, binding to ribosomes and stimulating translation.[30] This effect was observed in various systems, including an archaeon, yeast cells, and mammalian extracts, suggesting a conserved mechanism of action. Due to its exclusive mitochondrial localization, no interaction between the $tRNA^{Thr}$-3′-half and cytosolic ribosomes can take place in PCF. *In vitro* and *in vivo* binding studies demonstrate that mitochondrial $tRNA^{Thr}$-3′-halves interact with mitoribosomes (Figures 3B, 3D, and S3). Although ribosomes are highly conserved, a certain degree of variability exists. Kinetoplasts' mitoribosomes represent an extreme example of this variability, containing the smallest known rRNAs (40% of the bacterial rRNA content), compensated by an increase in the number of proteins, the highest described so far.[11] It is therefore remarkable that this functional tDR/ribosome interaction is conserved in so distantly related translation machineries.

The mitoribosome-bound $tRNA^{Thr}$-3′-half stimulates organellar protein synthesis during stress recovery (Figures 4C and 4D). Conversely, blocking the endogenous $tRNA^{Thr}$-3′-half via ASO led to a decrease in mitochondrial protein biosynthesis (Figures 4C and 4D). Notably, several subunits of the NADH dehydrogenase are encoded in the mitochondrial genome[45,46] and their activity can be tested using the MTT assay.[39,47] Upon electroporation of the $tRNA^{Thr}$-3′-half into mitochondria (Figure S4A), we observed a significant increase in MTT reduction, consistent with a role of the $tRNA^{Thr}$-3′-half in mitochondrial translation stimulation (Figure 4E).

Although the $tRNA^{Thr}$-3′-half stimulates mitochondrial translation, no significant increase in the incorporation of *de novo* synthesized subunits into mitochondrial OXPHOS complexes was observed nor did we see changes in mitochondrial membrane potential and total ATP levels (Figure S4C). In procyclic *T. brucei,* the mitochondrion contributes to most of the cell ATP levels[48] only if the cell relies on alternative carbon sources such as L-proline.[49] When cells are grown in glucose-rich media, L-proline metabolism is repressed, and parasites fulfill their energy requirements primarily through substrate-level phosphorylation.[50] Under these conditions, changes in mitochondrial translation would not be directly reflected in overall ATP levels. OXPHOS is an essential driver of mitochondrial membrane potential. If oxidative phosphorylation is not the primary source of energy generation, we would not expect to see any differences in the mitochondrial membrane potential, as was echoed by our TMRE staining assays (Figure S4C). Importantly, several subunits of the OXPHOS system are encoded in the nucleus. The coordinated expression of both nuclear and mitochondrial genes is crucial for the assembly of OXPHOS complexes. We cannot, therefore, rule out that the $tRNA^{Thr}$-3′-half stimulates the translation of only the mitochondrially encoded subunits while having no effect on the nuclear-encoded ones, eventually resulting in no net changes in the OXPHOS complexes levels. Despite all that, the $tRNA^{Thr}$-3′-half has a beneficial effect on the parasite's survival during stress recovery. When the endogenous $tRNA^{Thr}$-3′-half was blocked by ASO, the mortality rate significantly increases (Figure 4F).

Trypanosomes exposed to starvation produce many mitochondrial tDRs by a yet unknown mitochondrially localized RNase. The $tRNA^{Thr}$-3′-half reported here stimulates mitochondrial function, particularly organellar translation during stress recovery. Functionally, the $tRNA^{Thr}$-3′-half associates with mitoribosomes and acts as a rancRNA stimulating mitochondrial translation in trypanosomes.

Limitations of the study

We acknowledge several limitations of our study. First, we only investigated the changes driven by a single tRNA fragment, the $tRNA^{Thr}$-3′-half. Several tRNA fragments are present in cells exposed to stress, interestingly mainly inside mitochondria, and the crosstalk between them might coordinate cellular responses in more complex ways. Another limitation is the lack of information on the molecular mechanism driving mitochondrial translation stimulation. Currently, we can only speculate that, as previously described for cytosolic translation stimulation, the $tRNA^{Thr}$-3′-half facilitates mRNA loading onto ribosomes during stress recovery.[30] Furthermore, despite numerous attempts, we were unable to identify the enzyme responsible for tRNA fragmentation. At this point, we cannot exclude the possibility that redundant enzymes function in the generation of tDRs, further complicating any experimental approach. A key question

is whether tDR generation is a specific process and, if it is, how the specificity and regulation of the tRNA-cleaving enzyme are achieved. Only the identification of the RNase will provide further insights into this topic.

Additionally, this study primarily focuses on *Trypanosoma brucei*, and comparative analyses using other systems could shed light on the conservation of tDRs and their implications in mitochondrial biology across species.

STAR★METHODS

Detailed methods are provided in the online version of this paper and include the following:

- KEY RESOURCES TABLE
- RESOURCE AVAILABILITY
  - Lead contact
  - Materials availability
  - Data and code availability
- EXPERIMENTAL MODEL AND STUDY PARTICIPANT DETAILS
- METHOD DETAILS
  - Cell growth and stress conditions
  - RNA isolation
  - Denaturing polyacrylamide gel electrophoresis and northern blot analyses
  - Western Blot analyses
  - tRNA half transcript, antisense oligos and its electroporation
  - Digitonin extraction
  - *In vitro* cleavage assay
  - Preparation of mitochondrial vesicles
  - Mitoribosome profiling and purification of the *T. brucei* mitoribosomes
  - Immunoprecipitation of mitoribosomes
  - Mitochondrial translation in procyclic *T. brucei*
  - *In vitro* filter binding studies
  - MTT assay
  - Mitochondrial membrane potential determination
  - Blue native PAGE
  - mRNA northern blot analysis
  - Purification and *in vitro* activity of EndoV
- QUANTIFICATION AND STATISTICAL ANALYSIS

SUPPLEMENTAL INFORMATION

Supplemental information can be found online at https://doi.org/10.1016/j.celrep.2023.113112.

ACKNOWLEDGMENTS

We thank Salvatore Calderaro and Moritz Niemann for their help in purifying mitochondria. Ruslan Aphasizhev and Larry Simpson are thanked for the anti-KRET1 antibodies and Achim Schnaufer for the anti-KREL1 antibody. Manfred Heller from the Proteomics and Mass Spectrometry Core Facility (University of Bern) is acknowledged for MS data analyses.

This work was primarily supported by the NCCR RNA and Disease (grant number 182880). Additional support from the Swiss National Science Foundation grants 31003A_188969 (to N.P.) is acknowledged.

AUTHOR CONTRIBUTIONS

Conceptualization: N.P. and M.C.; Methodology: R.B. and M.C.; Validation: R.B., M.C., A.S., and N.P.; Formal analysis: R.B., M.C., A.S., and N.P.; Investigation: R.B. and M.C.; Resources: A.S. and N.P.; Writing – original draft: R.B.; Writing – review & editing: R.B., M.C., A.S., and N.P.; Visualization: R.B.; Supervision: N.P.; Funding acquisition: N.P.

DECLARATION OF INTERESTS

The authors declare no competing interests.

Received: March 30, 2023
Revised: July 7, 2023
Accepted: August 24, 2023

REFERENCES

1. Picard, M., McEwen, B.S., Epel, E.S., and Sandi, C. (2018). An energetic view of stress: Focus on mitochondria. Front. Neuroendocrinol. *49*, 72–85. https://doi.org/10.1016/j.yfrne.2018.01.001.
2. Boczonadi, V., and Horvath, R. (2014). Mitochondria: Impaired mitochondrial translation in human disease. Int. J. Biochem. Cell Biol. *48*, 77–84. https://doi.org/10.1016/j.biocel.2013.12.011.
3. Bennett, C.F., Latorre-Muro, P., and Puigserver, P. (2022). Mechanisms of mitochondrial respiratory adaptation. Nat. Rev. Mol. Cell Biol. *23*, 817–835. https://doi.org/10.1038/s41580-022-00506-6.
4. Balsa, E., Soustek, M.S., Thomas, A., Cogliati, S., García-Poyatos, C., Martín-García, E., Jedrychowski, M., Gygi, S.P., Enriquez, J.A., and Puigserver, P. (2019). ER and Nutrient Stress Promote Assembly of Respiratory Chain Supercomplexes through the PERK-eIF2α Axis. Mol. Cell *74*, 877–890.e6. https://doi.org/10.1016/j.molcel.2019.03.031.
5. Vonlaufen, N., Kanzok, S.M., Wek, R.C., and Sullivan, W.J., Jr. (2008). Stress response pathways in protozoan parasites. Cell Microbiol. *10*, 2387–2399. https://doi.org/10.1111/j.1462-5822.2008.01210.x.
6. Preußer, C., Jaé, N., and Bindereif, A. (2012). MRNA splicing in trypanosomes. Int. J. Med. Microbiol. *302*, 221–224. https://doi.org/10.1016/j.ijmm.2012.07.004.
7. Clayton, C. (2019). Regulation of gene expression in trypanosomatids: living with polycistronic transcription. Open Biol. *9*, 190072. https://doi.org/10.1098/rsob.190072.
8. Günzl, A. (2010). The pre-mRNA splicing machinery of trypanosomes: Complex or simplified? Eukaryot. Cell *9*, 1159–1170. https://doi.org/10.1128/EC.00113-10.
9. Aphasizheva, I., and Aphasizhev, R. (2016). U-Insertion/Deletion mRNA-Editing Holoenzyme: Definition in Sight. Trends Parasitol. *32*, 144–156. https://doi.org/10.1016/j.pt.2015.10.004.
10. Hashem, Y., des Georges, A., Fu, J., Buss, S.N., Jossinet, F., Jobe, A., Zhang, Q., Liao, H.Y., Grassucci, R.A., Bajaj, C., et al. (2013). High-resolution cryo-electron microscopy structure of the Trypanosoma brucei ribosome. Nature *494*, 385–389. https://doi.org/10.1038/nature11872.
11. Ramrath, D.J.F., Niemann, M., Leibundgut, M., Bieri, P., Prange, C., Horn, E.K., Leitner, A., Boehringer, D., Schneider, A., and Ban, N. (2018). Evolutionary shift toward protein-based architecture in trypanosomal mitochondrial ribosomes. Science *362*, eaau7735. https://doi.org/10.1126/science.aau7735.
12. Shikha, S., Brogli, R., Schneider, A., and Polacek, N. (2019). TRNA biology in trypanosomes. Chimia *73*, 395–405. https://doi.org/10.2533/chimia.2019.395.
13. Holmes, A.D., Chan, P.P., Chen, Q., Ivanov, P., Drouard, L., Polacek, N., Kay, M.A., and Lowe, T.M. (2023). A standardized ontology for naming tRNA-derived RNAs based on molecular origin. Nat. Methods *20*, 627–628. https://doi.org/10.1038/s41592-023-01813-2.

14. Polacek, N., and Ivanov, P. (2020). The regulatory world of tRNA fragments beyond canonical tRNA biology. RNA Biol. *17*, 1057–1059. https://doi.org/10.1080/15476286.2020.1785196.

15. Cristodero, M., and Polacek, N. (2017). The multifaceted regulatory potential of tRNA-derived fragments. Noncoding. RNA Investig. *1*, 7. https://doi.org/10.21037/ncri.2017.08.07.

16. Yamasaki, S., Ivanov, P., Hu, G.F., and Anderson, P. (2009). Angiogenin cleaves tRNA and promotes stress-induced translational repression. J. Cell Biol. *185*, 35–42. https://doi.org/10.1083/JCB.200811106.

17. Ivanov, P., Emara, M.M., Villen, J., Gygi, S.P., and Anderson, P. (2011). Angiogenin-Induced tRNA Fragments Inhibit Translation Initiation. Mol. Cell *43*, 613–623. https://doi.org/10.1016/J.MOLCEL.2011.06.022.

18. Lyons, S.M., Gudanis, D., Coyne, S.M., Gdaniec, Z., and Ivanov, P. (2017). Identification of functional tetramolecular RNA G-quadruplexes derived from transfer RNAs. Nat. Commun. *8*, 1127. https://doi.org/10.1038/s41467-017-01278-w.

19. Lyons, S.M., Achorn, C., Kedersha, N.L., Anderson, P.J., and Ivanov, P. (2016). YB-1 regulates tiRNA-induced Stress Granule formation but not translational repression. Nucleic Acids Res. *44*, 6949–6960. https://doi.org/10.1093/nar/gkw418.

20. Emara, M.M., Ivanov, P., Hickman, T., Dawra, N., Tisdale, S., Kedersha, N., Hu, G.F., and Anderson, P. (2010). Angiogenin-induced tRNA-derived stress-induced RNAs promote stress-induced stress granule assembly. J. Biol. Chem. *285*, 10959–10968. https://doi.org/10.1074/jbc.M109.077560.

21. Kim, H.K., Xu, J., Chu, K., Park, H., Jang, H., Li, P., Valdmanis, P.N., Zhang, Q.C., and Kay, M.A. (2019). A tRNA-Derived Small RNA Regulates Ribosomal Protein S28 Protein Levels after Translation Initiation in Humans and Mice. Cell Rep. *29*, 3816–3824.e4. https://doi.org/10.1016/j.celrep.2019.11.062.

22. Kim, H.K., Fuchs, G., Wang, S., Wei, W., Zhang, Y., Park, H., Roy-Chaudhuri, B., Li, P., Xu, J., Chu, K., et al. (2017). A tRNA-derived small RNA regulates ribosome biogenesis. Nature *552*, 57–62. https://doi.org/10.1038/NATURE25005.

23. Durdevic, Z., Mobin, M.B., Hanna, K., Lyko, F., and Schaefer, M. (2013). The RNA Methyltransferase Dnmt2 Is Required for Efficient Dicer-2-Dependent siRNA Pathway Activity in Drosophila. Cell Rep. *4*, 931–937. https://doi.org/10.1016/J.CELREP.2013.07.046.

24. Kuscu, C., Kumar, P., Kiran, M., Su, Z., Malik, A., and Dutta, A. (2018). tRNA fragments (tRFs) guide Ago to regulate gene expression post-transcriptionally in a Dicer-independent manner. RNA *24*, 1093–1105. https://doi.org/10.1261/RNA.066126.118.

25. Luo, S., He, F., Luo, J., Dou, S., Wang, Y., Guo, A., and Lu, J. (2018). Drosophila tsRNAs preferentially suppress general translation machinery via antisense pairing and participate in cellular starvation response. Nucleic Acids Res. *46*, 5250–5268. https://doi.org/10.1093/NAR/GKY189.

26. Pecoraro, V., Rosina, A., and Polacek, N. (2022). Ribosome-Associated ncRNAs (rancRNAs) Adjust Translation and Shape Proteomes. Noncoding. RNA *8*, 22. https://doi.org/10.3390/ncrna8020022.

27. Rajan, K.S., Doniger, T., Cohen-Chalamish, S., Rengaraj, P., Galili, B., Aryal, S., Unger, R., Tschudi, C., and Michaeli, S. (2020). Developmentally Regulated Novel Non-coding Anti-sense Regulators of mRNA Translation in Trypanosoma brucei. iScience *23*, 101780. https://doi.org/10.1016/j.isci.2020.101780.

28. Gebetsberger, J., Wyss, L., Mleczko, A.M., Reuther, J., and Polacek, N. (2017). A tRNA-derived fragment competes with mRNA for ribosome binding and regulates translation during stress. RNA Biol. *14*, 1364–1373. https://doi.org/10.1080/15476286.2016.1257470.

29. Gonskikh, Y., Gerstl, M., Kos, M., Borth, N., Schosserer, M., Grillari, J., and Polacek, N. (2020). Modulation of mammalian translation by a ribosome-associated tRNA half. RNA Biol. *17*, 1125–1136. https://doi.org/10.1080/15476286.2020.1744296.

30. Fricker, R., Brogli, R., Luidalepp, H., Wyss, L., Fasnacht, M., Joss, O., Zywicki, M., Helm, M., Schneider, A., Cristodero, M., and Polacek, N. (2019). A tRNA half modulates translation as stress response in Trypanosoma brucei. Nat. Commun. *10*, 118. https://doi.org/10.1038/s41467-018-07949-6.

31. Steinberg, S., Misch, A., and Sprinzl, M. (1993). Compilation of tRNA sequences and sequences of tRNA genes. Nucleic Acids Res. *21*, 3011–3015. https://doi.org/10.1093/nar/21.13.3011.

32. Hancock, K., and Hajduk, S.L. (1990). The mitochondrial tRNAs of Trypanosoma brucei are nuclear encoded. J. Biol. Chem. *265*, 19208–19215. https://doi.org/10.1016/S0021-9258(17)30645-2.

33. Niemann, M., and Schneider, A. (2020). A Scalable Purification Method for Mitochondria from Trypanosoma brucei. Trypanosomatids: Methods and Protocols, 611–626. https://doi.org/10.1007/978-1-0716-0294-2_36.

34. Thompson, D.M., and Parker, R. (2009). The RNase Rny1p cleaves tRNAs and promotes cell death during oxidative stress in Saccharomyces cerevisiae. J. Cell Biol. *185*, 43–50. https://doi.org/10.1083/jcb.200811119.

35. Nebohácová, M., Maslov, D.A., Falick, A.M., and Simpson, L. (2004). The Effect of RNA Interference Down-regulation of RNA Editing 3′-Terminal Uridylyl Transferase (TUTase) 1 on Mitochondrial de Novo Protein Synthesis and Stability of Respiratory Complexes in Trypanosoma brucei. J. Biol. Chem. *279*, 7819–7825. https://doi.org/10.1074/jbc.M311360200.

36. Cristodero, M., Mani, J., Oeljeklaus, S., Aeberhard, L., Hashimi, H., Ramrath, D.J.F., Lukeš, J., Warscheid, B., and Schneider, A. (2013). Mitochondrial translation factors of Trypanosoma brucei: Elongation factor-Tu has a unique subdomain that is essential for its function. Mol. Microbiol. *90*, 744–755. https://doi.org/10.1111/mmi.12397.

37. Kramer, S., Queiroz, R., Ellis, L., Webb, H., Hoheisel, J.D., Clayton, C., and Carrington, M. (2008). Heat shock causes a decrease in polysomes and the appearance of stress granules in trypanosomes independently of eIF2(alpha) phosphorylation at Thr169. J. Cell Sci. *121*, 3002–3014. https://doi.org/10.1242/jcs.031823.

38. Cristodero, M., Brogli, R., Joss, O., Schimanski, B., Schneider, A., and Polacek, N. (2021). tRNA 3′ shortening by LCCR4 as a response to stress in Trypanosoma brucei. Nucleic Acids Res. *49*, 1647–1661. https://doi.org/10.1093/nar/gkaa1261.

39. Huet, O., Petit, J.M., Ratinaud, M.H., and Julien, R. (1992). NADH-dependent dehydrogenase activity estimation by flow cytometric analysis of 3-(4,5-dimethylthiazolyl-2-yl)-2,5-diphenyltetrazolium bromide (MTT) reduction. Cytometry *13*, 532–539. https://doi.org/10.1002/cyto.990130513.

40. Dewar, C.E., Oeljeklaus, S., Mani, J., Mühlhäuser, W.W.D., von Känel, C., Zimmermann, J., Ochsenreiter, T., Warscheid, B., and Schneider, A. (2022). Mistargeting of aggregation prone mitochondrial proteins activates a nucleus-mediated posttranscriptional quality control pathway in trypanosomes. Nat. Commun. *13*, 3084. https://doi.org/10.1038/s41467-022-30748-z.

41. Shaukat, A.-N., Kaliatsi, E.G., Stamatopoulou, V., and Stathopoulos, C. (2021). Mitochondrial tRNA-Derived Fragments and Their Contribution to Gene Expression Regulation. Front. Physiol. *12*, 729452. https://doi.org/10.3389/fphys.2021.729452.

42. Shapiro, R., and Vallee, B.L. (1987). Human placental ribonuclease inhibitor abolishes both angiogenic and ribonucleolytic activities of angiogenin. Proc. Natl. Acad. Sci. USA *84*, 2238–2241. https://doi.org/10.1073/PNAS.84.8.2238.

43. Thompson, D.M., and Parker, R. (2009). Stressing out over tRNA cleavage. Cell *138*, 215–219. https://doi.org/10.1016/j.cell.2009.07.001.

44. García-Caballero, D., Pérez-Moreno, G., Estévez, A.M., Ruíz-Pérez, L.M., Vidal, A.E., and González-Pacanowska, D. (2017). Insights into the role of endonuclease V in RNA metabolism in Trypanosoma brucei. Sci. Rep. *7*, 1–15. https://doi.org/10.1038/s41598-017-08910-1.

45. Schneider, A. (2001). Unique aspects of mitochondrial biogenesis in trypanosomatids. Int. J. Parasitol. *31*, 1403–1415. https://doi.org/10.1016/S0020-7519(01)00296-X.

46. Kannan, S., and Burger, G. (2008). Unassigned MURF1 of kinetoplastids codes for NADH dehydrogenase subunit 2. BMC Genom. *9*, 455. https://doi.org/10.1186/1471-2164-9-455.

47. Berridge, M.v., and Tan, A.S. (1993). Characterization of the Cellular Reduction of 3-(4,5-dimethylthiazol-2-yl)-2,5-diphenyltetrazolium bromide (MTT): Subcellular Localization, Substrate Dependence, and Involvement of Mitochondrial Electron Transport in MTT Reduction. Arch. Biochem. Biophys. *303*, 474–482. https://doi.org/10.1006/ABBI.1993.1311.

48. Bochud-Allemann, N., and Schneider, A. (2002). Mitochondrial Substrate Level Phosphorylation Is Essential for Growth of Procyclic Trypanosoma brucei. J. Biol. Chem. *277*, 32849–32854. https://doi.org/10.1074/JBC.M205776200.

49. Besteiro, S., Barrett, M.P., Rivière, L., and Bringaud, F. (2005). Energy generation in insect stages of Trypanosoma brucei: metabolism in flux. Trends Parasitol. *21*, 185–191. https://doi.org/10.1016/J.PT.2005.02.008.

50. Lamour, N., Rivière, L., Coustou, V., Coombs, G.H., Barrett, M.P., and Bringaud, F. (2005). Proline Metabolism in Procyclic Trypanosoma brucei Is Down-regulated in the Presence of Glucose. J. Biol. Chem. *280*, 11902–11910. https://doi.org/10.1074/JBC.M414274200.

51. Wirtz, E., Leal, S., Ochatt, C., and Cross, G.A. (1999). A tightly regulated inducible expression system for conditional gene knock-outs and dominant-negative genetics in Trypanosoma brucei. Mol. Biochem. Parasitol. *99*, 89–101. https://doi.org/10.1016/S0166-6851(99)00002-X.

52. Schimanski, B., Nguyen, T.N., and Günzl, A. (2005). Highly Efficient Tandem Affinity Purification of Trypanosome Protein Complexes Based on a Novel Epitope Combination. Eukaryot. Cell *4*, 1942–1950. https://doi.org/10.1128/EC.4.11.1942-1950.2005.

53. Pusnik, M., Schmidt, O., Perry, A.J., Oeljeklaus, S., Niemann, M., Warscheid, B., Lithgow, T., Meisinger, C., and Schneider, A. (2011). Mitochondrial Preprotein Translocase of Trypanosomatids Has a Bacterial Origin. Curr. Biol. *21*, 1738–1743. https://doi.org/10.1016/j.cub.2011.08.060.

54. Chomczynski, P., and Sacchi, N. (1987). Single-step method of RNA isolation by acid guanidinium thiocyanate-phenol-chloroform extraction. Anal. Biochem. *162*, 156–159. https://doi.org/10.1006/ABIO.1987.9999.

55. Gebetsberger, J., Zywicki, M., Künzi, A., and Polacek, N. (2012). TRNA-derived fragments target the ribosome and function as regulatory noncoding RNA in Haloferax volcanii. Archaea *2012*, 10–12. https://doi.org/10.1155/2012/260909.

56. Aphasizhev, R., Sbicego, S., Peris, M., Jang, S.H., Aphasizheva, I., Simpson, A.M., Rivlin, A., and Simpson, L. (2002). Trypanosome Mitochondrial 3′ Terminal Uridylyl Transferase (TUTase): The Key Enzyme in U-Insertion/Deletion RNA Editing. Cell *108*, 637–648. https://doi.org/10.1016/S0092-8674(02)00647-5.

57. Schnaufer, A., Wu, M., Park, Y.J., Nakai, T., Deng, J., Proff, R., Hol, W.G.J., and Stuart, K.D. (2010). A protein-protein interaction map of trypanosome ~20s editosomes. J. Biol. Chem. *285*, 5282–5295. https://doi.org/10.1074/JBC.M109.059378/ATTACHMENT/50BEE33C-40DB-472C-A378-B5FD7A0DA365/MMC1.PDF.

58. Erlacher, M.D., Chirkova, A., Voegele, P., and Polacek, N. (2011). Generation of chemically engineered ribosomes for atomic mutagenesis studies on protein biosynthesis. Nat. Protoc. *6*, 580–592. https://doi.org/10.1038/nprot.2011.306.

59. Schneider, A., Charrière, F., Pusnik, M., and Horn, E.K. (2007). Isolation of Mitochondria from Procyclic Trypanosoma brucei. Mitochondria: Practical Protocols, 67–80. https://doi.org/10.1007/978-1-59745-365-3_5.

STAR★METHODS

KEY RESOURCES TABLE

REAGENT or RESOURCE	SOURCE	IDENTIFIER
Antibodies		
Polyclonal rabbit antibody anti-archaic translocase of the outer membrane 40	Andre Schneider	N/A
anti-*L. tarentolae* KRET1 antibody	Ruslan Aphasizhev	N/A
anti-*T. brucei* KREL1	Achim Schnaufer	N/A
mouse anti-HA antibody	Covance	Cat# MMS-101R, RRID: AB_2314672
mouse anti-EF1a	Santa Cruz	Cat# CBP-KK1, RRID: AB_668878
goat anti-mouse 680LT	Licor Biosciences	Cat# 926–68020, RRID: AB_10706161
goat anti-rabbit 800CW	Licor Biosciences	Cat# 926–32211, RRID: AB_621843
mouse anti-protein C	GenScript	Cat# A01774, RRID: AB_2744686
Chemicals, peptides, and recombinant proteins		
IgG Sepharose Fast Flow	GE Healthcare	Cat# GE17-0969-01
Puromycin	Sigma Aldrich	Cat# P7255
Cycloheximide	Carl Roth	Cat# 8682
Digitonin	Sigma Aldrich	Cat# D141
Thiazolyl Blue tetrazolium bromide	Thermo Scientific	Cat# L11939.03
Critical commercial assays		
TMRE Mitochondrial Membrane Potential kit	Abcam	Cat# ab113852
Experimental models: Organisms/strains		
Trypanosoma brucei Lister 427 Procyclic form	George Cross Rockefeller Univ. NY.	N/A
Trypanosoma brucei 29-13 Procyclic form	George Cross Rockefeller Univ. NY.	N/A
Trypanosoma brucei 19-3 Procyclic form	André Schneider	N/A
Trypanosoma brucei NYSM Bloodstream form	George Cross Rockefeller Univ. NY.	N/A
Oligonucleotides		
See Table S1	This paper	N/A
Software and algorithms		
FlowJo	BD Biosciences	https://www.flowjo.com/solutions/flowjo RRID:SCR_008520
ImageQuant TL analysis software	Cytiva	https://www.cytivalifesciences.com/en/us/shop/protein-analysis/molecular-imaging-for-proteins/imaging-software/imagequant-tl-10-2-analysis-software-p-28619#order
ImageJ	https://imagej.net/	RRID:SCR_003070
Microsoft Excel	https://office.microsoft.com/excel	RRID:SCR_016137
Other		
NovoCyte Flow cytometer system	Agilent	N/A
Tecan plate reader	Tecan	N/A
Typhoon laser scanner	Cytiva	N/A

RESOURCE AVAILABILITY

Lead contact

Further information and requests for resources and reagents should be directed to and will be fulfilled by the lead contact, Marina Cristodero (marina.cristodero@unibe.ch).

Materials availability

This study did not generate new unique reagents.

Data and code availability

- All data reported in this paper will be shared by the lead contact upon request.
- This study does not report original code.
- Any additional information required to reanalyze the data reported in this paper is available from the lead contact upon request.

EXPERIMENTAL MODEL AND STUDY PARTICIPANT DETAILS

Trypanosoma brucei procyclic stage (PCF) Lister 427, 29-13[51] and bloodstream forms New York single markers (BSF) cell lines were used in all experiments.

METHOD DETAILS

Cell growth and stress conditions

Procyclic stage cells Lister 427 and 29-13 were grown at 27°C in SDM-79 media complemented with 5% (v/v) and 10% (v/v) Fetal bovine serum (FBS), respectively. Bloodstream forms (BSF) were cultured in HMI-9 medium supplemented with 10% FBS at 37°C/ 5% CO_2. Exponentially growing PCF *T. brucei* cells were harvested at a density of 1-2 x 10^7 cells/mL and 10^6/mL for BSF.

Nutritional stress was applied to PCF cells by incubating them for 2 h in 1 x PBS (Phosphate buffered saline) at 27°C and for BSF cells 1 h in 1 x PBS at 37°C. For stress recovery PCF cells were grown in full media for 1 to 2 h at 27°C dependent on the experimental setup.

The cell line used for affinity purification of mitoribosomes contains one allele coding for the mitoribosomal protein uL3m (Tb927.3.5610) tagged *in situ* at the C terminus with a sequence containing a tandem affinity tag. The tag consists of the protein A and protein C epitopes separated by a cleavage site for the tobacco edge virus protease (PTP-tag).[11,52]

The inducible EndoV RNAi cell line was done by amplifying the region encompassing bases 28 to 363 using oligos 274_acgAAGCTTGGATCCGCGATAAAGTTGGACATG and 275_ ctTCTAGACTCGAGGCCCGCCTCCCGGAACG and cloned it in a modified pLew100 vector containing the blasticidin resistance gene.[48] The tetracycline-inducible ATOM40 RNAi and EF-Tu RNAi cell lines were generated using the same strategy and backbone vector, and have been previously described.[36,53] Induction of RNAi was done by the addition of tetracycline (1 μg/mL; Sigma-Aldrich). Tetracycline-inducible expression of C-terminally HA-tagged EndoV (Tb927.10.6860) was done using pLew100-derived constructs carrying the puromycin resistance marker and three copies of the HA epitope. The complete EndoV ORF was amplified using oligos 276_acgAAGCTTATGGGTGTGGGAGAAATGAG and 277_agctCTC GAGGCATTCATTTAGTTGAATCCGTC. The constructs were transfected in 427-derived BS19.3 expressing the T7 RNA polymerase and the Tet repressor from a stably integrated plasmid.

RNA isolation

T. brucei total RNA was isolated using Tri-reagent (*Zymo Research*) according to the manufacturer's instructions and RNA derived from *in vitro* cleavage reactions was isolated by phenol/chloroform/isoamyl alcohol extraction.

For RNA extractions from sucrose fractions, a hot phenol method was used. 40 μL of 10% SDS was added to a 400 μL sucrose fraction. The suspension was vortexed and an equal volume of prewarmed acid phenol (pH 4.3) (*Sigma Aldrich*) was added. The mixture was vortexed again and incubated at 65°C for 5 min. Then 200 μL of chloroform (*Fluka*) was added and shortly vortexed. The mixture was then rapidly chilled on ice for 5 min and centrifuged at 12′000 RPM at RT for 5 min. The upper phase was extracted with phenol/chloroform/isoamyl alcohol (Roth), and RNA precipitated with ethanol. After washing with 70% of ethanol, the pellet was dried and resuspended in 10 μL of 1x RNA loading dye.

RNA extraction after digitonin fractionation was performed using acidic phenol/chloroform extraction in the presence of 4 M guanidinium isothiocyanate, 0.5% (w/v) sodium N-lauroylsarcosinate and 100 mM β-mercaptoethanol.[54]

Denaturing polyacrylamide gel electrophoresis and northern blot analyses

For denaturing polyacrylamide gel electrophoresis between 3 and 40 μg RNA in 1x RNA loading dye was separated on a 4%, 8% or 12% denaturing polyacrylamide gel (7M Urea, in 1x TBE buffer) dependent on the resolution required. To visualize the RNA, the gel was incubated with ethidium bromide (EtBr) in electrophoresis buffer containing 0.5 μg/mL of EtBr. If subsequent northern blot analyses were performed the gel was electroblotted onto a nylon membrane (Amersham Hybond N^+, *GE Healthcare*) and hybridized as described.[55] The sequences of the DNA probes used are listed in Table S1.

Western Blot analyses

For Western blot analysis total cell lysates (corresponding to 2-3 x 10^6 cells), fractions obtained during digitonin fractionation (corresponding to 2-3 x 10^6 cells) or sucrose gradient fractions 20 μL (400 μL total volume per fraction) were mixed with 2x Laemmli

buffer, denatured at 95°C for 2 min and separated in 10% or 12% SDS-PAGE gels. The gel was transferred onto a nitrocellulose membrane (*Amersham Biosciences*) and blocked for 1h in 1x PBS supplemented with 0.1% Tween 20 (PBST) containing 5% nonfat milk. The membrane was incubated with primary antibodies: polyclonal rabbit antibody anti-archaic translocase of the outer membrane 40 (ATOM40) (dilution 1:10′000); anti-*L. tarentolae* KRET1 antibody (dilution 1:500, kindly provided by Ruslan Aphasizhev and Larry Simpson[56]; anti-KREL1 (dilution 1:100) antibody kindly provided by Achim Schnaufer,[57] mouse anti-HA antibody (1:5000, Covane), mouse anti-EF1a (1:10′000, Santa Cruz). Membranes were washed (3 × 10 min each with PBST) after overnight incubation at 4°C. Secondary antibodies (anti-mouse 680LT and anti-rabbit 800 CW; *Li-Cor Biosciences*) were used at a dilution of 1: 20′000. Blots were scanned using the Li-Cor Odyssey Clx infrared imaging system. All antibody dilutions were done in 1x PBST containing 2.5% (w/v) milk.

tRNA half transcript, antisense oligos and its electroporation

To generate $tRNA^{Thr}$-3′-half (without CCA tail) *in vitro* the template was first generated by PCR using overlapping oligos: IVT: $tRNA^{Thr}$ half fw and IVT $tRNA^{Thr}$ half rev. The clean PCR product was used as a template for *in vitro* transcription by T7 RNA polymerase as described in[58] resulting in the following transcript: Thr_(AGU)-3′-half-CCA: 5′ AAGACGGAGGUCGGGGGUUCGAUCCCCCCAGU GGCCU 3′

For tDR-5′-Ala we used a synthetic oligonucleotide (*Microsynth*) with the sequence Ala_(CGA)-5′-half: 5′GGGGAUGUAGC UCAGAUGGUAGAGCGCCCGCUUAGC 3′. To block endogenous $tRNA^{Thr}$-3′-halves we used modified antisense oligos ASO_a: mG*mA*mA*mC*mC*C*C*C*C*G*A*C*C*T-*C*C*mG*mT*mC*mT*mT and ASO_b mA*mG*mG*mC*mC*A*C*T*G*G*G*G*G*A* mT*mC*mG *mA*mA (*Qiagen*).

500 pmol of *in vitro* transcribed synthetic RNA transcripts or antisense oligos to block endogenous $tRNA^{Thr}$-3′-halves were electroporated into exponentially growing PCF cells as previously described.[30] Briefly, 4.5 × 10^7 procyclic cells were harvested by centrifugation (1,400 xg for 10 min at 4°C), washed once with 1 mL of ice-cold Cytomix (25 mM HEPES/KOH pH 7.6, 10 mM K_2HPO_4, 120 mM KCl, 0.15 mM $CaCl_2$, 5 mM $MgCl_2$, 2 mM EDTA), resuspended in 190 μL 1x Cytomix and mixed with 500 pmol of *in vitro* transcribed tRNA half in 1x annealing buffer (10 mM Tris-HCl; pH 7.6, 80 mM $MgCl_2$) to a final volume of 200μL. The mixture was electroporated twice using a Bio-Rad gene pulser II (1.2 kV, 25 μF, and 0 Ohm) in a 4 mm electroporation cuvette (EP-104, Cell Projects Ltd.). Finally, cells were resuspended with 1 mL of SDM-79 (5% FCS) and transferred into 3 mL of pre-warmed medium for a 2 h recovery at 27°C. To assess the efficiency of electroporation into mitochondria, electroporated cells were fractionated using digitonin as described and the presence of the $tRNA^{Thr}$-3′-halves in the different fractions was investigated by northern blot analysis. A calibration curve was done by loading different amounts of the *in vitro* transcribed $tRNA^{Thr}$-3′-half in the same gel.

Digitonin extraction

Digitonin extraction was used to generate crude mitochondrial fractions for mitochondrial lysate generation, enrichment for mitochondrial translation products, and BN-PAGE analysis. For this 10^8 procyclic cells were resuspended in 0.5 mL of SoTE (0.6 M sorbitol, 20 mM Tris-HCl, pH 7.5, 2 mM EDTA) and 0.5 mL of SoTE containing 0.03% (w/v) digitonin was added, and the sample was mixed and incubated on ice for 5 min to selectively solubilize the plasma membrane. Centrifugation (5 min, 6,800 xg, 4°C) yielded a cytosol-enriched supernatant and a mitochondria-enriched pellet. 2 × 10^6 cell equivalents of each fraction were subjected to SDS-PAGE and immunoblotting. Alternatively, for tRNA subcellular localization analysis, mitochondrial pellets were resuspended in 500 μL of SoTE containing 1 μg of RNase A and incubated on ice for 15 min. After the final centrifugation, the supernatants were discarded, and RNA was extracted with guanidinium isothiocyanate as described above.

In vitro cleavage assay

Exponential growing cells or gradient purified mitochondria were harvested and the cell pellets (1-2 x 10^9) resuspended in 500 μL ribosome buffer A (120 mM KCl, 20 mM Tris/HCl pH 7.6, 2 mM $MgCl_2$, 1 mM DTT) and 2.5 μL of RNasin (40 U/Lμ, *Promega*) and flash frozen. Samples were passed 10 times through a 25G needle and 10 times through a 27G needle and extracts were cleared by centrifugation.

To test the activity of the tDR-generating enzyme between 10 and 40 μL (corresponding to 2-8 × 10^7 cells) of total cell or mitochondrial lysate were used. To the mitochondrial lysate, 5 μg of total RNA was supplemented. The lysates were incubated for 30 min at 30°C in 1x ribosome buffer A. As a negative control, lysates were not incubated but immediately processed. Total RNA was extracted with ROTI Aqua-P/C/I (*Roth*) and northern blot analyses were performed. Inhibition experiments of total cell lysates were performed in the presence of different concentrations of ribonucleoside vanadyl complex (VRC, *Bioconcept*).

Preparation of mitochondrial vesicles

Isolation and purification of mitochondrial vesicles were performed from 4 to 6 L of exponentially growing 1-3 x 10^7 427 Lister *T. brucei cells* WT or 427 Lister cells containing an *in situ* tagged mitoribosome protein (uL3m, Tb927.3.5610) as described.[11,33,59] Briefly, cells were grown in 2 L Erlenmeyer flasks shaking at 120 rpm and 27°C. Nitrogen cavitation was performed at 70 bar for 45–60 min at a cell density of ∼2.5 × 10^9 cells/mL in 1X SoTE buffer. The mitochondrial fraction was harvested via centrifugation (16′000 rpm, 10 min, 4°C, Sorvall SS-34 rotor) and genomic DNA was degraded using DNase I (100 μg/mL, 20–30 min, 0°C). The remaining cells and debris were removed by centrifuging in 50 mL Falcon tubes (555 xg, 20 min, 4°C). The mitochondrial vesicles

were harvested from the supernatant as described above and resuspended in 1X SoTE buffer containing 50% (w/v) Nycodenz. Nycodenz step gradients (18/21/25/28% (w/v) Nycodenz in 1X SoTE buffer; capacity 3.5-8 x 10^{10} cells) were underlaid with the vesicle suspension and the gradients were centrifuged at 27′000 rpm for 45 min at 4°C (Beckman Coulter SW32 Ti). Mitochondrial vesicles were harvested from the second band from the top appearing at the 21/25% (w/v) Nycodenz interface. A typical yield at this scale was around 50 mg of mitochondrial protein as determined by the bicinchoninic acid (BCA) assay. Samples corresponding to different purification steps were collected. The protein concentration was determined by BCA assay. Northern blot analyses and western blotting with 5 μg of each sample was performed as described above. Besides the already mentioned antibodies: mouse anti-protein C (dilution 1:3′000, HPC4, GenScript) and mouse anti-elongation factor 1a (EF1a) (dilution 1:10′000 Santa cruz) were used to check the purity of the fractions.

Mitoribosome profiling and purification of the *T. brucei* mitoribosomes

Approximately 1–1.5 g (wet weight) corresponding to 2 to 3 mL purified mitochondrial vesicles in 1 XSoTE were lysed in equal volume of lysis buffer (5 mM Na_2H/NaH_2PO_4 pH 7.4, 40 mM HEPES-KOH pH 7.4, 10 mM $Mg(CH_3COO)_2$, 30 mM KCl, 2 mM dithiothreitol (DTT), 2% (w/v) n-dodecyl b–D-maltoside (DDM), 125 μM spermidine, 125 μM spermine, 1 x of complete protease inhibitor cocktail (*Roche*) and 20 U/mL RNasin (40 U/μL *Promega*)) for 40 min at 4°C by continuous mixing. The mitochondrial lysate was cleared by two centrifugation steps at 12,000 rpm for 25 min at 4°C. 400 μL of cleared supernatant was loaded on 500 μL (60% w/v) sucrose in resuspension buffer (5 mM Na_2H/NaH_2PO_4 pH 7.4, 40 mM HEPES-KOH pH 7.4, 10 mM $Mg(CH_3COO)_2$, 30 mM KCl, 2 mM DTT, 0.01% (w/v) DDM, 125 μM spermidine, 125 μM spermine, 1 x of complete protease inhibitor cocktail (*Roche*) and 20 U/mL Ribolock (40 U/μL *Thermo Scientific)*) and ultracentrifuged in a Sorvall M120+ miniultracentrifuge equipped with an S140AT rotor (*Thermo Scientific,* 65,000 rpm, 20 h, 4°C). The obtained supernatant (mitS100) was used for subsequent WB controls and the mitochondrial pellet (mitP100) containing high molecular weight complexes such as mitoribosomes and editosomes was resuspended in 500 μL 1x resuspension buffer. OD_{260} was measured and equal amounts (5–10 OD_{260} units) were layered on a 10–35% sucrose gradient prepared in Resuspension buffer and centrifuged (40,000 rpm, 2 h 15 min, 4°C, in SW41Ti Beckman Coulter, Brea, CA, US). Gradients were pumped out and fractionated into 30 equal fractions, which were tested by Western blot and northern blot analysis. To purify mitoribosomes for filter binding assays, fractions containing the mitoribosomes were collected and buffer-exchanged to resuspension buffer in a tabletop centrifuge at 4°C using centrifugal filters (Amicon) until the sucrose concentration was lower than 1%.

To test binding of *in vitro* transcribed $tRNA^{Thr}$-3′-halves to mitoribosomes 100 pmol of *in vitro* transcribed $tRNA^{Thr}$-3′-halves were incubated with 10 OD_{260} units mitP100 for 30 min at 30°C. mitP100 was split in two and to one sample, EDTA (f.c 50 mM) was added to dissociate the mitoribosomes. Sucrose gradient fractionation was performed as described above.

Immunoprecipitation of mitoribosomes

450 μL mitochondrial vesicles from cells expressing *in situ* PTP tagged uL3m mitoribosomal protein, were lysed and mitP100 in 1x resuspension buffer was generated as earlier described. The mitP100 lysate was incubated with pre-washed IgG Sepharose (*Healthcare*). After 2 h of rotation, the beads were washed twice with resuspension buffer. To confirm successful immunoprecipitation 2% of post-mitoribosomal supernatant (mitS100), of the mitoribosome-enriched pellet (mitP100), and of the flow-through of the purification (FT) and 5% of the bead-bound fraction (Bound) were tested by Western blot using anti-protein C antibody, anti-KREL1 (mitochondrial RNA editing ligase 1, component of the RECC complex) antibody, and anti-ATOM40 antibody. RNA was extracted from the beads, input and flow-through sample and northern blot analyses were performed. For this 5% of mitP100 and FT, and 80% of the bound fraction (Bound) were used while the 12S mitochondrial rRNA serves as a marker for mitochondrial ribosomes.

Mitochondrial translation in procyclic *T. brucei*

Per mitochondrial translation reaction three times 4.5 × 10^7 procyclic *T. brucei* cells were electroporated as already described,[30] each with 500 pmol of Thr_(AGU)-3′-half -CCA or modified antisense oligos (ASO_a & ASO_b). After a 2 h recovery from electroporation, cells were starved in 1x PBS for 2 h. Cells were then counted, and 10^7 cells were recovered for 1 h in 1 mL SDM-79 under normal growth conditions. All the cells were harvested at 800 x g for 1 min and washed with SoTE buffer (0.6 M sorbitol, 20 mM Tris-HCl, pH 7.5, 2 mM EDTA). To inhibit cytosolic translation 10^7 cells were incubated for 5 min with cycloheximide (f.c. 100 μg/mL) and metabolic labeling was performed using 100 μCi per reaction (10 μL) Met-^{35}S-Label (L-Methionine ^{35}S (73%) + L-Cysteine ^{35}S (22%), 10 mCi/mL, *Hartmann Analytic*) for 1 h at 27°C. When indicated, the reactions were performed in the presence of puromycin (f.c 100 μg/mL). To enrich for mitochondrial proteins digitonin extraction and solubilization (see above) were performed and finally, the mitochondria-enriched pellet was resuspended in 50 μL of 2x Laemmli Buffer. For normalization, 5 μL of mitochondria-enriched pellet (corresponding to 10^6 cells) of each translation reaction were run on a 10% SDS-PAGE and stained with Coomassie. The protein content per lane was quantified using ImageJ and used as a loading reference to ensure equal loading of translation reactions on the 2D Gels. Samples were further analyzed by two-dimensional Tris-glycine SDS gels with a 9% gel in the first dimension (5 h; max 10 W). Each lane was cut out and incubated for 1 h at 37°C in a denaturing solution (1% SDS, 125 mM Tris-HCl, pH 6.8, 1% β-mercaptoethanol) before loading the gel piece on the second dimension

14% Tris-glycine SDS gel (15 h, 90 V max 10 W). The 2D gels were fixed and stained in Coomassie. For autoradiography, dried gels were exposed to a phosphor-imager screen and analyzed using a PhosphorImager.

Stock solutions of the antibiotics were prepared at 100 mg/mL in water for puromycin (*Sigma Aldrich*) or at 100 mg/mL in ethanol for cycloheximide (*Carl Roth*).

In vitro filter binding studies

Binding studies of $tRNA^{Thr}$-3′-halves to procyclic *T. brucei* ribosomal and mitoribosomal particles were performed using a dot blot-filtering approach. For the filter binding assay 0.1 pmol of *T. brucei* cytosolic or mitochondrial ribosomes were incubated with increasing amounts of 5′-^{32}P-end-labeled $tRNA^{Thr}$-3′-half from 0.1 pmol/μL to 1 pmol/μL in 25 μL of SoTE for 30 min at 27°C. After incubation, the reactions were filtered through a nitrocellulose membrane (0.45 μM diameter) using a vacuum device, followed by 2 washing steps with ice-cold SoTE buffer. Membranes were exposed to phosphorimaging screens and analyzed with a phosphoimager.

For 5′ radiolabeling the tRNA halves were phosphorylated using polynucleotide kinase and gamma ^{32}P-ATP. 80S ribosomes were isolated from exponentially growing cells as already described[30] and 50S mitoribosomes (as described above).

MTT assay

Procyclic exponential growing *T. brucei* cells were electroporated empty (Mock) or with tRNA halves. After electroporation, cells were allowed to recover for 1 h in SDM-79 media containing 5% FBS. 2×10^6 cells were harvested and resuspended in 100 μL full media. 10 μL of 12 mM MTT prepared in 1x PBS was added to each sample. A sample with only media served as a negative control. Cells were incubated for 2 h in a 96-well plate (*Merck*) in a shaking incubator (220 rpm, 30°C). To stop the reaction 100 μL of SDS-HCl (1 g SDS in 10 mL 0.1 M HCl) was added, mixed, and incubated for 12 h. Absorbance was measured at 570 nm with a Tecan plate reader.

Mitochondrial membrane potential determination

The TMRE Mitochondrial Membrane Potential kit (*Abcam*) was used. Procyclic *T. brucei* cells were electroporated empty (Mock), with $tRNA^{Thr}$-3′-halves or antisense oligonucleotides (ASO) to block endogenous $tRNA^{Thr}$-3′-halves and allowed to recover for 2 h in full media. Afterward, cells were stressed for 2 h in PBS and 1×10^6 cells were put into 1 mL of full media to recover (1 h, 600 rpm, 27°C). During the second hour of recovery, 1×10^5 cells were supplemented with 100 nM TMRE and left shaking at 30°C for 20 min. As a negative control, cells were preincubated with 20 μM FCCP for 10 min or with cycloheximide (f.c 100 μg/mL). *T. brucei* cells were washed three times in 0.2% BSA + 1x PBS containing 6 mM glucose (PBSG) and resuspended in 500 μL of 0.2% BSA in PBSG, left for 30 min protected from light. Cells were analyzed in a Novocyte instrument (Agilent), using the 488 nm laser for excitation and detected using the B586/20nm filter. Data were analyzed using FlowJo.

Blue native PAGE

To test if newly synthesized mitochondrial proteins are incorporated into mitochondrial respiratory complexes, an *in vivo* mitochondrial translation assay was performed followed by BN-PAGE. Digitonin-extracted mitochondria-enriched pellet was solubilized for 15 min in solubilization buffer containing 1% (w/v) digitonin, 20mM Tris-HCl pH 7.4, 50mM NaCl, 5% glycerol, 0.05 mM EDTA to solubilize mitochondrial membranes. The mitochondrial lysate was cleared by centrifugation (15 min, 20,817 xg, 4°C) and finally, the samples were separated on a 4–13% acrylamide gradient gels for 1D BN-PAGE. Radiolabeled methionine/cysteine incorporation was measured by phosphorimaging.

mRNA northern blot analysis

5 μg of total RNA were separated on a 1% agarose gel in 20 mM MOPS buffer, pH 7.0, containing 0.5% formaldehyde. The probes used for the Northern blot analysis were generated from gel-purified PCR products corresponding to the RNAi targeting region and radioactively labeled using the Prime-a-Gene labeling kit (*Promega*).

Purification and *in vitro* activity of EndoV

To test tRNA fragmentation activity cells expressing HA-tagged EndoV were tetracycline induced or left untreated (mock) for 2 days. After this, the cells were stressed with 1 x PBS for 2 h. To purify the tagged EndoV, cells were washed with 1 x PBS and resuspended in lysis buffer (20 mM Tris pH 7.7, 3 mM $MgCl_2$, 0.1% NP40, 1 mM DTT and 20 mM KCl) containing protease inhibitors (*Roche*) at a density of 10^9 cells/mL of lysis buffer. After 5 min incubation on ice KCl was added to a final concentration of 150 mM, the lysate was centrifuged for 15 min at maximal speed and then incubated with pre-washed anti HA beads (*Roche*). After 2 h of rotation at 4°C the beads were washed with lysis buffer containing 150 mM KCl, then with the same buffer containing 500 mM KCl, and finally washed with ribosome buffer A and resuspended in the same buffer. To determine the amount of bead-bound protein to be used in the reaction a fraction of the beads was boiled in Laemmli buffer and tested by Western blot analysis using anti HA antibodies. Equal amounts of bead-bound EndoV-HA were incubated with 5 μg of total RNA purified from exponentially growing cells. Reactions

were incubated at 30°C and after the indicated time points beads were removed by centrifugation. Finally, RNA was extracted using phenol/chloroform, precipitated, resuspended in RNA loading buffer, separated on 12% polyacrylamide/urea gels, and analyzed by northern blot.

QUANTIFICATION AND STATISTICAL ANALYSIS

Northern blot signals were obtained using Phosphorimager screens, scanned in a Typhoon scanner (Cytiva), and analyzed using ImageQuant TL analysis software (Cytiva). Coomassie signals were quantified using ImageJ.

For autoradiography, dried gels were exposed to Phosphorimager screens, scanned in a Typhoon scanner (Cytiva), and analyzed using ImageQuant TL analysis software (Cytiva).

For MTT assays, absorbance was measured at 570 nm using a Tecan plate reader.

Mitochondrial membrane potential was investigated using the TMRE assay. Fluorescent cells were analyzed in a Novocyte instrument (Agilent), using the 488 nm laser for excitation and detected using the B586/20nm filter. Data were analyzed using FlowJo.

All statistical analyses were done using Microsoft Excel.